Environmental Earth Sciences (2020) 79:155
https://doi.org/10.1007/s12665-020-8893-9

ORIGINAL ARTICLE

Effects of slope and flow depth on the roughness coefficient of lodged vegetation

Shengtang Zhang[1] · Ying Liu[1] · Zhikai Wang[1] · Guibao Li[1] · Si Chen[1] · Ming Liu[1]

Received: 6 December 2018 / Accepted: 1 March 2020 / Published online: 18 March 2020

Abstract

Various vegetations are often grown on floodplains, and it has a significant influence on the movement of water flow and the protection of river slopes. In the experiments performed in this study, a cylindrical aluminum column with a diameter of 4 mm was selected to simulate natural vegetation and 7 classes of slopes ($i = 0\%$, 0.5%, 1.0%, 1.5%, 2.0%, 2.5%, and 3.0%, where i is the percentage of slope) and four categories of lodging angles ($\theta = 20°$, 40°, 60°, and 80°) were assigned. The experimental results show that when $i > 0\%$, the curves of Manning's roughness coefficient (n) and flow depth (h) converge, and the degree of convergence gradually increases with the slope. In addition, Manning's roughness coefficient increases with the increase in slope at shallow flow depths, and decreases with the increase in slope at deeper flow depths. Exploration of the relationship between slope and vegetation roughness not only provides a theoretical support for flood control, but also has practical significance for river ecological environment management.

Keywords Lodged vegetation · Slope · Manning's roughness coefficient · Overland runoff

Introduction

In the river ecosystem, the influence of vegetation cannot be neglected. Vegetation has a stabilizing effect on riverbeds, defends the hirsts and dikes, and protects and rests ecological environment, but at the same time, vegetation can increase the roughness of banks and change the flow regime, thus affecting the flood diversion capacity of the river (Carroll et al. 1997; Cerdà 1997; Fattet et al. 2011; Zhao et al. 2017; Liu et al. 2018). Aquatic vegetation is prone to lodging under the flow of water, and there are many factors that induce the lodging of vegetation. In addition to intrinsic factors, such as the flexibility and overall structure of the vegetation, the slope is also one of the most important factors affecting the lodging of vegetation. Studying the relationship between slope and lodged vegetation roughness not only provides theoretical support for flood control, but also has practical implications in river ecological environment management.

While there have been many studies on the vegetation roughness on slopes (e.g., Abrahams and Parsons 1994; Atkinson et al. 2000), there have been few on vegetation lodging. Among them, Ferro et al. (2005) showed that vegetation flow resistance decreases with an increase in slope, although the relationship is complex, and cannot be expressed by a simple function. Han et al. (2016) examined the non-uniform distribution of flexible, submerged vegetation in a rectangular channel and concluded that the mean velocity decreased with increasing flow resistance. Meanwhile, Velasco et al. (2003) used simulated plastic plants instead of real plants in flume experiments, and the relationship between the deflected height of flexible plants and the velocity field was measured. They found that plant roughness correlated directly with the lodging deformation of plants. Busari and Li (2015) estimated the uncertainty of a hydraulic roughness model of submerged flexible vegetation,

✉ Shengtang Zhang
zst0077@163.com

Ying Liu
liuying5128@126.com

Zhikai Wang
wangzhikai666@126.com

Guibao Li
liguibao1127@163.com

Si Chen
Chensi9604@163.com

Ming Liu
liuying5128@126.com

[1] College of Earth Science and Engineering, Shandong University of Science and Technology, Qingdao, China

and suggested that the hydraulic resistance produced by submerged flexible vegetation depends on many factors, including plant stem size, height, number, and density, as well as flow depth.

The research on the flow characteristics of vegetation accounted for a high percentage in the past (Cerdà 1997; Järvelä 2002; Yagci et al. 2010; Guo et al. 2016). According to vegetation characteristics, it can be divided into coverage area, flexibility, diameter, and leaf number on the basis of the prevailing research (Wilson et al. 2003; Kothyari et al. 2009; Hu et al. 2012). At present, the studies on the effects of slope on the hydrodynamic characteristics of overland runoff are becoming more advanced. However, studies on the hydrodynamic characteristics of lodged vegetation remain limited (Ferro et al. (2005)), especially with respect to the effect of slope on the flow roughness of lodged vegetation. Therefore, it is necessary to experimentally investigate the effects of changes in slope on the surface roughness of lodged vegetation. This provides a theoretical basis for further exploring the river flow structure and movement characteristics, and has practical significance for river ecological restoration and flood control.

Experimental setup

According to previous studies, it is necessary to perform open channel flow simulation experiments (e.g., through indoor simulations), and the data processing and theoretical research on the experiments should be performed using the formulae and theory of open channel flows. Furthermore, there are many factors that affect the flow resistance of vegetation. To clearly study changes in flow resistance under different lodging states, it was necessary to simplify the simulations in this study. Before formal testing, a preliminary experiment was performed to select the experimental materials and to determine the slope and lodging angle. In the indoor open-channel flow simulation, a plexiglass plate was positioned on the bottom of the instrument as the reference plane, and the angle of the vegetation from the vertical direction of the reference plane was used as the lodging angle. In addition, a cylindrical aluminum column (Hsieh 1964; Huthoff et al. 2007; Luo et al. 2009; Yagci et al. 2010; Zhu et al. 2018) with a diameter of 4 mm and a fixed height of 10 cm was used to simulate natural vegetation. Seven classes of slope (indicated by i, where $i = 0\%$, 0.5%, 1.0%, 1.5%, 2.0%, 2.5%, and 3.0%), and four categories of lodging angles (indicated by θ, where $\theta = 20°$, 40°, 60°, and 80°) were also used to perform the experiment.

Due to the large volume of water used in the test, and to conserve water resources, a device for recirculating water flow within the closed system was used. The device consisted of an open-channel flume with a rectangular section, a water tank, water pump, and a tailgate. During simulations, water flow could be pumped from the water tank into the open-channel flume, and then returned to the water tank through the test section to recycle the water (Fig. 1). The rectangular flume was 5 m long, 0.4 m wide at the bottom, and the side walls were 0.3 m in height. A plexiglass plate was placed on the bottom, and the surface was drilled with small holes at a longitudinal and lateral spacing of 60 mm × 60 mm for the placement of simulated vegetation. The flume was divided into three sections: an upper equalizing section (1 m in length), a middle test section (3 m in length), and a tailgate section (1 m in length). In the experimental section, two cross sections, 1 and 2, were put in place with a separation distance of 1.5 m, and both of them were equipped with piezometer tubes to observe water level. A steel beam was placed below the flume to adjust the slope, and the range in slope varied between 0 and 3%. A flow control valve was

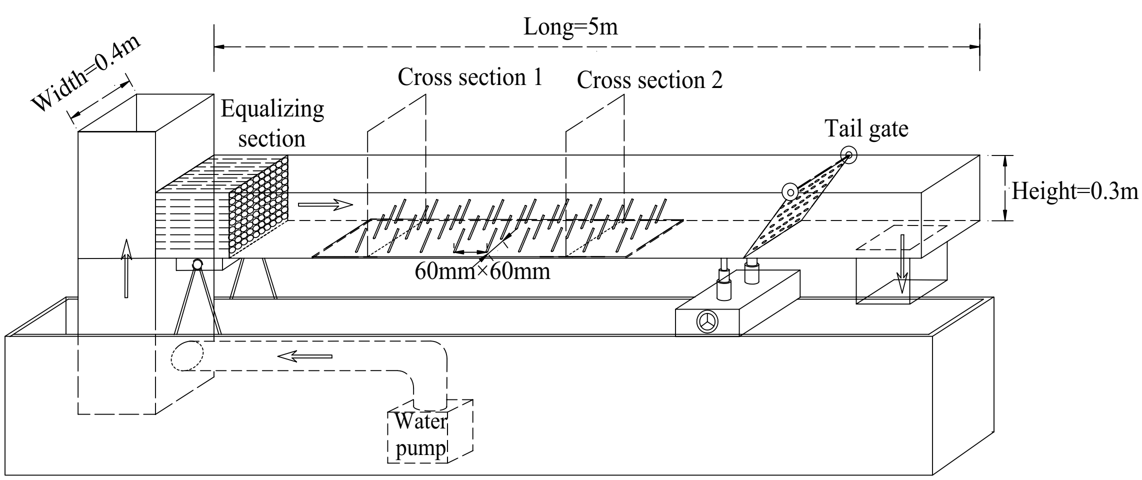

Fig. 1 Experimental setup for the monitoring of the effect of vegetation lodging

Table 1 Experimental data under different slopes (i=0%, 0.5%, 1.0%, 1.5%, 2.0%, 2.5%, and 3.0%) and lodging angles (θ=20°, 40°, 60°, and 80°)

Slope (%)	Lodging angle (θ)	Paramete r	Experiment number				
			1	2	3	4	5
0.0	20°	$h_c(m)$	0.0172	0.0320	0.0424	0.0515	0.0667
		$v(m/s)$	0.1163	0.1219	0.1394	0.1566	0.1831
		Re	1496	2738	3972	5220	7454
		n	0.0203	0.0239	0.0259	0.0290	0.0317
	40°	$h_c(m)$	0.0160	0.0280	0.0391	0.0489	0.0654
		$v(m/s)$	0.1254	0.1388	0.1513	0.1639	0.1848
		Re	1544	2843	4126	5371	7594
		n	0.0170	0.0203	0.0214	0.0237	0.0283
	60°	$h_c(m)$	0.0146	0.0288	0.0395	0.0491	0.0584
		$v(m/s)$	0.1274	0.1326	0.1516	0.1653	0.1745
		Re	1445	2787	4167	5429	6579
		n	0.0161	0.0199	0.0208	0.0215	0.0200
	80°	$h_c(m)$	0.0153	0.0289	0.0391	0.0484	0.0565
		$v(m/s)$	0.1186	0.1358	0.1515	0.1676	0.1776
		Re	1402	2851	4123	5440	6518
		n	0.0138	0.0150	0.0141	0.0121	0.0125
0.5	20°	$h_c(m)$	0.0107	0.0229	0.0332	0.0425	0.0506
		$v(m/s)$	0.1780	0.1698	0.1809	0.1898	0.1972
		Re	1541	2982	4397	5686	6804
		n	0.0172	0.0213	0.0240	0.0279	0.0325
	40°	$h_c(m)$	0.0104	0.0221	0.0319	0.0410	0.0497
		$v(m/s)$	0.1880	0.1815	0.1877	0.1964	0.2035
		Re	1592	3080	4409	5707	6924
		n	0.0162	0.0186	0.0216	0.0234	0.0268
	60°	$h_c(m)$	0.0104	0.0224	0.0322	0.0419	0.0501
		$v(m/s)$	0.1813	0.1761	0.1856	0.1942	0.1993
		Re	1498	2951	4292	5611	6653
		n	0.0161	0.0169	0.0187	0.0211	0.0228
	80°	$h_c(m)$	0.0089	0.0211	0.0298	0.0392	0.0478
		$v(m/s)$	0.2174	0.1892	0.1993	0.2065	0.2140
		Re	1577	3086	4408	5781	7050
		n	0.0148	0.0160	0.0155	0.0144	0.0155
1.0	20°	$h_c(m)$	0.0078	0.0155	0.0246	0.0334	0.0423
		$v(m/s)$	0.2433	0.2670	0.2576	0.2459	0.2425
		Re	1570	3269	4799	5992	7217
		n	0.0155	0.0186	0.0201	0.0225	0.0261
	40°	$h_c(m)$	0.0081	0.0146	0.0226	0.0323	0.0408
		$v(m/s)$	0.2569	0.2878	0.2872	0.2610	0.2548
		Re	1698	3331	4948	6177	7355
		n	0.0150	0.0173	0.0174	0.0209	0.0225
	60°	$h_c(m)$	0.0077	0.0153	0.0221	0.0317	0.0475
		$v(m/s)$	0.2483	0.2794	0.2972	0.2693	0.2597
		Re	1582	3368	5011	6261	8495
		n	0.0151	0.0179	0.0165	0.0174	0.0209

Table 1 (continued)

Slope (%)	Lodging angle (θ)	Paramete r	Experiment number				
			1	2	3	4	5
	80°	$h_c(m)$	0.0074	0.0142	0.0212	0.0280	0.0366
		$v(m/s)$	0.2580	0.2904	0.3185	0.3151	0.2913
		Re	1583	3280	5172	6553	7645
		n	0.0143	0.0174	0.0163	0.0143	0.0141
1.5	20°	$h_c(m)$	0.0070	0.0106	0.0184	0.0250	0.0312
		$v(m/s)$	0.2768	0.3701	0.3410	0.3566	0.3663
		Re	1635	3256	5019	6882	8544
		n	0.0158	0.0156	0.0217	0.0218	0.0205
	40°	$h_c(m)$	0.0067	0.0104	0.0174	0.0241	0.0298
		$v(m/s)$	0.2990	0.3885	0.3752	0.3752	0.3858
		Re	1468	2913	4537	6078	7504
		n	0.0143	0.0148	0.0198	0.0211	0.0200
	60°	$h_c(m)$	0.0068	0.0103	0.0178	0.0240	0.0297
		$v(m/s)$	0.2818	0.3761	0.3590	0.3862	0.3848
		Re	1630	3221	5122	7156	8596
		n	0.0153	0.0150	0.0206	0.0205	0.0198
	80°	$h_c(m)$	0.0068	0.0103	0.0159	0.0217	0.0325
		$v(m/s)$	0.2895	0.3729	0.3930	0.4031	0.4394
		Re	1662	3208	5062	6848	10,583
		n	0.0149	0.0150	0.0186	0.0202	0.0189
2.0	20°	$h_c(m)$	0.0060	0.0132	0.0203	0.0272	0.0381
		$v(m/s)$	0.3012	0.4521	0.4186	0.4090	0.4203
		Re	1742	5557	7624	9612	13,136
		n	0.0153	0.0170	0.0230	0.0253	0.0246
	40°	$h_c(m)$	0.0062	0.0121	0.0188	0.0250	0.0313
		$v(m/s)$	0.3269	0.4871	0.4570	0.4471	0.4464
		Re	1736	4871	6831	8602	10,423
		n	0.0146	0.0150	0.0209	0.0235	0.0241
	60°	$h_c(m)$	0.0060	0.0121	0.0194	0.0252	0.0304
		$v(m/s)$	0.3175	0.4944	0.4498	0.4534	0.4585
		Re	1634	4924	6934	8780	10,445
		n	0.0146	0.0143	0.0214	0.0233	0.0239
	80°	$h_c(m)$	0.0056	0.0112	0.0152	0.0218	0.0271
		$v(m/s)$	0.2977	0.5281	0.5469	0.5067	0.5116
		Re	1433	4886	6743	8641	10,557
		n	0.0149	0.0135	0.0160	0.0210	0.0225
2.5	20°	$h_c(m)$	0.0061	0.0094	0.0121	0.0150	0.0200
		$v(m/s)$	0.3131	0.4182	0.4921	0.5404	0.5165
		Re	1618	3299	4911	6598	8226
		n	0.0166	0.0164	0.0164	0.0172	0.0216
	40°	$h_c(m)$	0.0054	0.0086	0.0114	0.0138	0.0187
		$v(m/s)$	0.3631	0.4501	0.5192	0.5809	0.5566
		Re	1725	3328	5046	6755	8526
		n	0.0134	0.0143	0.0151	0.0152	0.0199
	60°	$h_c(m)$	0.0054	0.0088	0.0114	0.0135	0.0161
		$v(m/s)$	0.3441	0.4469	0.5204	0.5948	0.6223
		Re	1578	3310	4909	6604	8115
		n	0.0140	0.0148	0.0148	0.0144	0.0156

Table 1 (continued)

Slope (%)	Lodging angle (θ)	Paramete r	Experiment number				
			1	2	3	4	5
	80°	$h_c(m)$	0.0054	0.0084	0.0102	0.0125	0.0149
		$v(m/s)$	0.3770	0.4640	0.5745	0.6537	0.6885
		Re	1729	3269	4875	6753	8355
		n	0.0129	0.0135	0.0126	0.0129	0.0133
3.0	20°	$h_c(m)$	0.0055	0.0087	0.0111	0.0139	0.0192
		$v(m/s)$	0.3636	0.4430	0.5301	0.5853	0.6336
		Re	1750	3303	4992	6818	9957
		n	0.0148	0.0160	0.0158	0.0165	0.0186
	40°	$h_c(m)$	0.0052	0.0077	0.0110	0.0154	0.0180
		$v(m/s)$	0.3477	0.4215	0.5439	0.6557	0.6679
		Re	1611	2883	5208	8649	10,149
		n	0.0146	0.0154	0.0153	0.0155	0.0167
	60°	$h_c(m)$	0.0050	0.0084	0.0131	0.0171	0.0194
		$v(m/s)$	0.3567	0.4616	0.6128	0.7079	0.7374
		Re	1550	3327	6776	10,002	11,697
		n	0.0140	0.0152	0.0149	0.0152	0.0165
	80°	$h_c(m)$	0.0052	0.0083	0.0122	0.0145	0.0181
		$v(m/s)$	0.3982	0.4637	0.6481	0.6943	0.7801
		Re	1764	3220	6531	8226	11,316
		n	0.0138	0.0147	0.0139	0.0143	0.0152

Slope (%)	Lodging angle (θ)	Paramete r	Experiment number						
			6	7	8	9	10	11	12
0.0	20°	$h_c(m)$	0.0744	0.0815	0.0945	0.1054	0.1108	0.1152	0.1190
		$v(m/s)$	0.1915	0.2011	0.2161	0.2354	0.2434	0.2502	0.2543
		Re	8453	9480	11,290	13,227	14,130	14,895	15,446
		n	0.0331	0.0345	0.0354	0.0363	0.0355	0.0351	0.0336
	40°	$h_c(m)$	0.0740	0.0824	0.0930	0.1035	0.1093	0.1140	0.1182
		$v(m/s)$	0.1942	0.1983	0.2209	0.2385	0.2449	0.2526	0.2589
		Re	8745	9647	11,702	13,565	14,429	15,293	16,035
		n	0.0292	0.0302	0.0286	0.0277	0.0266	0.0262	0.0259
	60°	$h_c(m)$	0.0720	0.0786	0.0850	0.0905	0.1016	0.1126	0.1161
		$v(m/s)$	0.1969	0.2074	0.2169	0.2260	0.2429	0.2569	0.2601
		Re	8693	9755	10,784	11,742	13,647	15,428	15,928
		n	0.0180	0.0187	0.0185	0.0191	0.0209	0.0207	0.0207
	80°	$h_c(m)$	0.0637	0.0713	0.0840	0.0901	0.1012	0.1071	0.1159
		$v(m/s)$	0.1900	0.2002	0.2197	0.2280	0.2434	0.2499	0.2615
		Re	7661	8762	10,842	11,814	13,643	14,531	15,991
		n	0.0111	0.0111	0.0122	0.0109	0.0120	0.0107	0.0119
0.5	20°	$h_c(m)$	0.0581	0.0721	0.0866	0.0916	0.0969	0.1025	0.1105
		$v(m/s)$	0.2065	0.2250	0.2375	0.2461	0.2545	0.2624	0.2761
		Re	7948	10,190	12,270	13,218	14,195	15,193	16,795
		n	0.0351	0.0368	0.0370	0.0373	0.0367	0.0351	0.0342

Table 1 (continued)

Slope (%)	Lodging angle (θ)	Paramete r	Experiment number						
			6	7	8	9	10	11	12
	40°	$h_c(m)$	0.0573	0.0714	0.0836	0.0884	0.0942	0.1000	0.1080
		$v(m/s)$	0.2116	0.2288	0.2464	0.2548	0.2623	0.2672	0.2817
		Re	8056	10,290	12,417	13,347	14,358	15,219	16,887
		n	0.0314	0.0344	0.0324	0.0318	0.0299	0.0273	0.0264
	60°	$h_c(m)$	0.0574	0.0644	0.0764	0.0875	0.0932	0.0987	0.1069
		$v(m/s)$	0.2112	0.2210	0.2408	0.2582	0.2646	0.2711	0.2830
		Re	7849	8977	11,098	13,105	14,030	14,943	16,442
		n	0.0249	0.0247	0.0223	0.0206	0.0196	0.0196	0.0206
	80°	$h_c(m)$	0.0603	0.0671	0.0739	0.0801	0.0910	0.0961	0.1045
		$v(m/s)$	0.2334	0.2436	0.2486	0.2583	0.2721	0.2792	0.2897
		Re	9236	10,457	11,458	12,626	14,546	15,485	16,990
		n	0.0158	0.0153	0.0161	0.0141	0.0141	0.0141	0.0117
1.0	20°	$h_c(m)$	0.0509	0.0648	0.0777	0.0833	0.0892	0.0948	0.1036
		$v(m/s)$	0.2423	0.2539	0.2655	0.2737	0.2785	0.2845	0.2970
		Re	8385	10,610	12,692	13,748	14,681	15,627	17,315
		n	0.0312	0.0350	0.0369	0.0375	0.0372	0.0374	0.0370
	40°	$h_c(m)$	0.0486	0.0549	0.0624	0.0755	0.0857	0.0910	0.1003
		$v(m/s)$	0.2540	0.2581	0.2643	0.2727	0.2891	0.2955	0.3060
		Re	8468	9485	10,732	12,755	14,818	15,782	17,449
		n	0.0253	0.0282	0.0310	0.0324	0.0319	0.0307	0.0288
	60°	$h_c(m)$	0.0540	0.0608	0.0677	0.0729	0.0835	0.0885	0.0970
		$v(m/s)$	0.2641	0.2710	0.2771	0.2830	0.2975	0.3033	0.3134
		Re	9568	10,774	11,958	12,894	14,964	15,884	17,478
		n	0.0229	0.0245	0.0235	0.0227	0.0215	0.0204	0.0197
	80°	$h_c(m)$	0.0437	0.0503	0.0638	0.0695	0.0810	0.0863	0.0941
		$v(m/s)$	0.2853	0.2877	0.2928	0.2993	0.3085	0.3139	0.3301
		Re	8696	9846	12,067	13,163	15,174	16,148	18,025
		n	0.0150	0.0152	0.0160	0.0156	0.0154	0.0134	0.0111
1.5	20°	$h_c(m)$	0.0399	0.0477	0.0614	0.0735	0.0799	0.0852	0.0931
		$v(m/s)$	0.3231	0.3092	0.3043	0.3093	0.3125	0.3169	0.3266
		Re	9339	10,386	12,484	14,542	15,611	16,560	18,152
		n	0.0236	0.0275	0.0323	0.0354	0.0354	0.0361	0.0359
	40°	$h_c(m)$	0.0363	0.0452	0.0594	0.0716	0.0768	0.0827	0.0898
		$v(m/s)$	0.3703	0.3288	0.3172	0.3201	0.3269	0.3281	0.3375
		Re	8530	9145	10,996	12,795	13,757	14,561	15,872
		n	0.0191	0.0232	0.0280	0.0309	0.0319	0.0314	0.0306
	60°	$h_c(m)$	0.0353	0.0424	0.0576	0.0687	0.0743	0.0798	0.0879
		$v(m/s)$	0.3949	0.3637	0.3344	0.3359	0.3394	0.3416	0.3498
		Re	10,195	11,011	13,029	14,989	16,052	17,006	18,653
		n	0.0176	0.0169	0.0211	0.0226	0.0223	0.0212	0.0206
	80°	$h_c(m)$	0.0375	0.0408	0.0462	0.0558	0.0683	0.0745	0.0835
		$v(m/s)$	0.4479	0.4915	0.4765	0.3919	0.3744	0.3696	0.3702
		Re	12,149	14,216	15,296	14,825	16,589	17,481	19,024
		n	0.0171	0.0156	0.0118	0.0113	0.0131	0.0135	0.0149
2.0	20°	$h_c(m)$	0.0431	0.0515	0.0585	0.0649	0.0713	0.0771	0.0856
		$v(m/s)$	0.4244	0.3889	0.3693	0.3621	0.3571	0.3551	0.3620
		Re	14,682	15,611	16,451	17,504	18,534	19,536	21,470
		n	0.0235	0.0249	0.0284	0.0309	0.0331	0.0350	0.0357

Table 1 (continued)

Slope (%)	Lodging angle (θ)	Paramete r	Experiment number						
			6	7	8	9	10	11	12
	40°	$h_c(m)$	0.0417	0.0465	0.0546	0.0605	0.0670	0.0730	0.0820
		$v(m/s)$	0.4545	0.4592	0.4078	0.3923	0.3831	0.3796	0.3789
		Re	13,464	14,854	15,134	15,810	16,714	17,670	19,219
		n	0.0227	0.0210	0.0232	0.0255	0.0275	0.0288	0.0308
	60°	$h_c(m)$	0.0389	0.0437	0.0512	0.0556	0.0650	0.0717	0.0752
		$v(m/s)$	0.4987	0.5056	0.5341	0.5354	0.4523	0.4304	0.4239
		Re	13,916	15,501	18,523	19,825	19,132	19,665	20,088
		n	0.0226	0.0215	0.0190	0.0167	0.0149	0.0163	0.0166
	80°	$h_c(m)$	0.0364	0.0438	0.0480	0.0521	0.0555	0.0589	0.0624
		$v(m/s)$	0.5313	0.5758	0.5870	0.5956	0.6057	0.6142	0.6192
		Re	14,036	17,633	19,298	20,848	22,259	23,600	24,839
		n	0.0230	0.0221	0.0211	0.0200	0.0191	0.0177	0.0159
2.5	20°	$h_c(m)$	0.0278	0.0383	0.0520	0.0521	0.0565	0.0647	0.0753
		$v(m/s)$	0.4680	0.4914	0.4520	0.4963	0.4968	0.4474	0.4216
		Re	9920	13,610	16,002	17,610	18,772	18,907	20,028
		n	0.0270	0.0275	0.0261	0.0260	0.0247	0.0275	0.0317
	40°	$h_c(m)$	0.0254	0.0365	0.0424	0.0502	0.0578	0.0628	0.0676
		$v(m/s)$	0.5263	0.5260	0.4963	0.5219	0.5466	0.5276	0.4840
		Re	10,576	14,310	15,333	18,403	21,466	22,157	21,629
		n	0.0243	0.0265	0.0274	0.0259	0.0234	0.0226	0.0242
	60°	$h_c(m)$	0.0248	0.0300	0.0338	0.0422	0.0472	0.0540	0.0597
		$v(m/s)$	0.5262	0.5208	0.5590	0.5877	0.5914	0.6100	0.6169
		Re	10,107	11,776	13,942	17,486	19,233	22,007	24,033
		n	0.0240	0.0259	0.0258	0.0258	0.0254	0.0244	0.0231
	80°	$h_c(m)$	0.0196	0.0272	0.0305	0.0354	0.0425	0.0498	0.0558
		$v(m/s)$	0.6285	0.5683	0.6187	0.6317	0.6299	0.6548	0.6831
		Re	9828	11,830	14,131	16,288	18,917	22,205	25,263
		n	0.0184	0.0238	0.0242	0.0251	0.0258	0.0256	0.0251
3.0	20°	$h_c(m)$	0.0270	0.0338	0.0389	0.0437	0.0517	0.0559	0.0628
		$v(m/s)$	0.5488	0.5293	0.5367	0.5416	0.5538	0.5576	0.5584
		Re	11,677	13,617	15,459	17,139	19,974	21,378	23,399
		n	0.0264	0.0294	0.0300	0.0302	0.0296	0.0291	0.0281
	40°	$h_c(m)$	0.0255	0.0311	0.0360	0.0449	0.0491	0.0528	0.0588
		$v(m/s)$	0.5853	0.5924	0.5895	0.6058	0.6064	0.6115	0.6170
		Re	12,137	14,505	16,301	19,959	21,465	22,902	25,100
		n	0.0245	0.02680	0.0281	0.0287	0.0287	0.0285	0.0278
	60°	$h_c(m)$	0.0264	0.0324	0.0377	0.0413	0.0458	0.0500	0.0553
		$v(m/s)$	0.6558	0.6360	0.6286	0.6306	0.6322	0.6376	0.6588
		Re	13,668	15,727	17,618	19,019	20,715	22,349	24,906
		n	0.0234	0.0263	0.0278	0.0283	0.0287	0.0287	0.0282
	80°	$h_c(m)$	0.0205	0.0294	0.0372	0.0418	0.0464	0.0497	0.0518
		$v(m/s)$	0.8015	0.6798	0.6773	0.6833	0.6889	0.7025	0.7075
		Re	13,025	15,108	18,343	20,300	22,178	23,816	24,776
		n	0.0163	0.0243	0.0268	0.0277	0.0282	0.0283	0.0283

positioned at the connection point between the water tank and the open-channel flume, and the flow rate varied from 0 to 0.0125 m^3/s.

Theory and data

The roughness coefficient is one of the most important hydrodynamic parameters to understand as it indicates the roughness of the surface and the obstructive effects of vegetation on the flow of water (Barros and Colello 2001; Wang et al. 2014; Zhang et al. 2018). The primary means of expressing the roughness coefficient are the Manning, Darcy-Weisbach, and Chezy flow resistance equations (Rouhipour et al. 1999; Hogarth et al. 2005; Smith et al. 2007). Moreover, according to the experimental data processing, the minimum Reynolds number (Re; Eq. 1) was ~ 1400, which is much larger than the critical value of 500, meaning that the flow was in a turbulent state throughout the experiment. Therefore, the Manning's roughness coefficient (n; Eq. 2) was considered to be the most accurate parameter:

$$Re = \frac{vR}{\upsilon}, \tag{1}$$

where v is the mean velocity (m/s) between cross sections 1 and 2, R is the hydraulic radius (m), υ is kinematic viscosity (m^2/s), and

$$n = \frac{1}{v} R^{2/3} J^{1/2}, \tag{2}$$

where J is the hydraulic gradient (dimensionless), n is Manning's roughness coefficient ($s/m^{1/3}$) (Smith et al. 2007).

In the process of calculating the roughness coefficient, both the hydraulic radius and the hydraulic gradient are important parameters that affect the results. The hydraulic radius is the ratio of the area of flow passing through a water section to the boundary line (i.e., wet cycle) of the contact between the fluid and the solid wall (Eq. 3; Querner 1997; Cheng and Nguyen 2011; Vatankhah et al. 2015). Meanwhile, the hydraulic gradient is the head loss *per* unit distance along the water flow path (Eq. 4; Zheng et al. 2000; Heuperman 2007; Nouwakpo et al. 2010), such that

$$R = \frac{A}{\chi}, \tag{3}$$

where A is the cross-sectional area of water flow (m^2) and χ is the wetted perimeter (m):

$$J = \frac{h_f}{l}, \tag{4}$$

where h_f is the frictional head loss (m) and l is the length of water along the course (m).

Fig. 2 Relationships between Manning's roughness coefficient (n) and flow depth (h) under different lodging angles and slopes (**a** $i = 0.0\%$; **b** $i = 0.5\%$; **c** $i = 1.0\%$; **d** $i = 1.5\%$; **e** $i = 2.0\%$; **f** $i = 2.5\%$; **g** $i = 3.0\%$), the hollow points stand for submersed and the filled points for unsubmersed vegetation ▶

During the experiment, we measured the pressure with piezometer tubes in Sects. 1 and 2, and recorded the flow depths and flow velocities as h_1, h_2, v_1, and v_2, respectively. The flow depth (h_c), current velocity (v), and the hydraulic radius (R) were calculated using the mean values of cross sections 1 and 2 (i.e., $h_c = (h_1 + h_2)/2$; $= v(v_1 + v_2)/2$; $R = (R_1 + R_2)/2$). The formulae for calculating the current velocities of each cross section are shown in Eq. 5:

$$v_1 = \frac{Q}{Bh_1}; v_2 = \frac{Q}{Bh_2} \tag{5}$$

where v_1 is the current velocity and h_1 is the flow depth for cross section 1, v_2 is the current velocity and h_2 is the flow depth for cross section 2, B is the channel width (m), and Q is the flow rate (m^3/s).

Four categories of lodging angles (20°, 40°, 60°, and 80°) were used in the experiment, and 7 classes of slopes were assigned to each angle (where $i = 0\%$ indicates horizontality; $i = 0.5\%$ and 1.0% indicate a shallow slope; $i = 1.5\%$ and 2.0% indicate a medium slope; $i = 2.5\%$ and 3.0% indicate a steep slope). During the experiment, the flow rate (Q) and the water depth (h_c) corresponding to different slopes, (i), and different lodging angles, (θ), were measured, and then the corresponding Manning's roughness coefficient (n)was calculated using Eq. 2; the results are shown in Table 1.

Results and discussion

The relationships between the Manning's roughness coefficient (n) and water depth (h) calculated under different experimental slopes are shown in (Fig. 2). Figure 2a shows the n–h relationship for a horizontal state (i.e., with $i = 0\%$). When the vegetation is at the same lodging angle, the Manning's roughness coefficient (n) increases gradually as the water depth (h) increases, before gradually decreasing. The reason for this behavior may be that with increasing water depth, the degree of submergence of the vegetation increases, causing the area of water blockage to increases. Under these circumstances, the Manning's roughness coefficient (n) exhibits an increasing trend. When the vegetation is completely submerged, as the water depth increases and the water blocking area does not change, the resistance generated by the vegetation does not change, but the water depth continues to increase. Compared to the unsubmerged state, the Manning's roughness coefficient (n) shows a decreasing

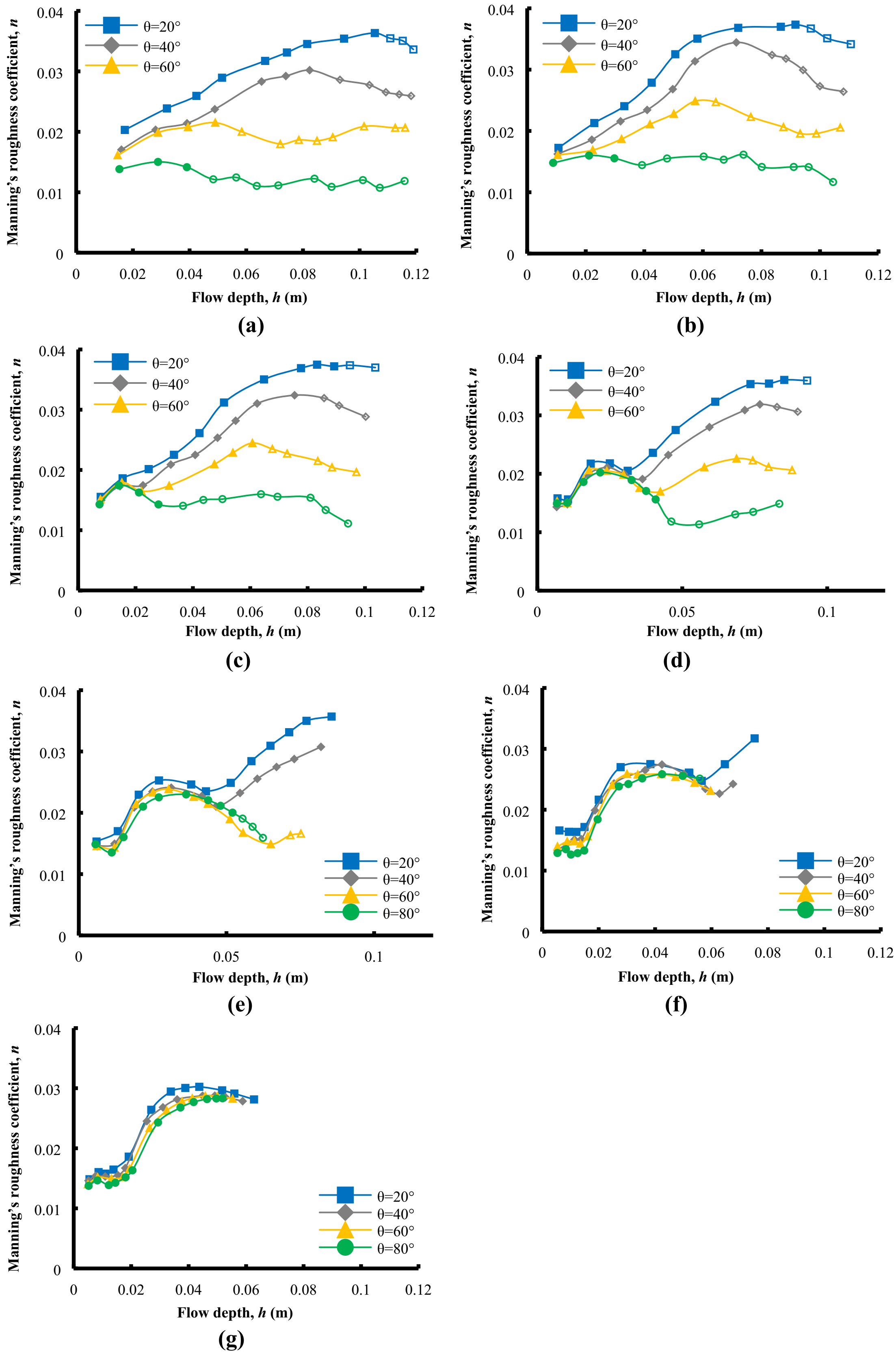

Manning's roughness coefficient, n
Flow depth, h (m)
θ=20°
θ=40°
θ=60°
θ=80°
(a)
(b)
(c)
(d)
(e)
(f)
(g)

trend. Under the same water depth, as the lodging angle (θ) increases, the Manning's roughness coefficient (n) gradually decreases in the order of: $n_{20°} > n_{40°} > n_{60°} > n_{80°}$. This may be because with an increasing degree of lodging, the vertical projection of the vegetation, which has a fixed height, decreases gradually, and the area of water blockage decreases accordingly; thus, the Manning's roughness coefficient (n) exhibits a decreasing trend.

Figure 2b, c shows the relationships of n–h under shallow slope conditions ($i=0.5\%$ and 1.0%). It can be seen from the figures that, compared with the horizontal state, the n–h curves at shallow water depths and for shallow slopes just begin to converge with one other, and the n–h curves at greater water depths do not change significantly. From this pattern, we infer that shallow slopes can only affect the size of the Manning's roughness coefficient (n) for lodged vegetation under shallow water depths. Figure 2d, e shows the relationship of n–h for medium slopes ($i=1.5\%$ and 2.0%). Compared to the horizontal and shallow slope states, the n–h curves with medium slopes are obviously closer; the n–h curves at shallow water depths remain converged, and the n–h curves at greater water depths begin to converge. Finally, Fig. 2f, g shows the relationship of n–h with steep slopes ($i=2.5\%$ and 3.0%). It can be seen from these figures that whether at deep or shallow water depths, the n–h curves almost completely converge for all lodging angles, especially for the steepest slope ($i=3\%$), as shown in Fig. 2g.

The general trends shown in Fig. 2 are that of convergence in the relationship of n–h as the slope increases, and that the water depth that can be achieved under the same flow conditions decreases with increasing slope. The reason for this phenomenon may be that the Manning's roughness coefficient (n) of vegetation was mainly controlled by three factors during the experiment: the lodging angle (θ), slope (i), and water depth (h). In the horizontal state, the Manning's roughness coefficient (n) of the vegetation is not affected by the slope, and the lodging angle is the main controlling factor. As the slope gradually increases, the influence on Manning's roughness coefficient (n) increases, and gradually exhibits a greater influence than the lodging angle (θ) until the slope (i) becomes the dominant factor (Fig. 2g). In the process of the slope effect increasing and the influence of the lodging angle decreasing, water depth is an important criterion. Under the conditions of a shallow slope, only the hydraulic characteristics under shallow water depths are affected by the slope, and with an increase in slope, the affected water depth increases gradually.

Therefore, the lodging angle is fixed at 20° to observe the relationship between Manning's roughness coefficient (n) and water depth (h) on different slopes, as shown in Fig. 3. It can be seen from the figure that with increasing water depth, the Manning's roughness coefficient (n) for different slopes generally increases. This is because for unsubmerged vegetation,

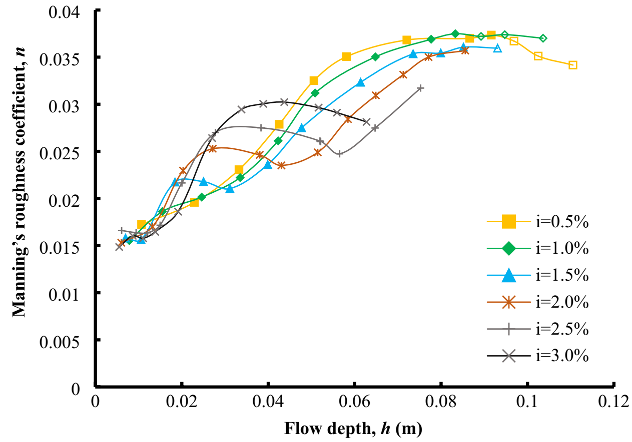

Fig. 3 Relationship between Manning's roughness coefficient (n) and flow depth (h) for different slopes when the lodging angle is 20°, the hollow points stand for submersed and the filled points for unsubmersed vegetation

with increasing water depth, the degree in vegetation submergence increases, and the area of water blockage also increases, thus increasing the Manning's roughness coefficient (n). In addition, under the same water depth, the Manning's roughness coefficient (n) is positively correlated with slope at shallow water depths ($0 < h < 0.05$ m), but negatively correlated with slope at greater water depths ($0.05 < h < 0.11$ m). Therefore, through comparative study, it can be concluded that the flow resistance generated by vegetation is closely related to the slope, the lodging angle, and the water depth.

Conclusions

Vegetation is one of the important components of river ecosystems. To further study the effect of vegetation roughness on water flow, open-channel flow simulation experiments were carried out. The following conclusions were drawn:

1. When $i=0\%$, the Manning's roughness coefficient (n) increases gradually as the water depth (h) increases at the same lodging angle (θ), and then gradually decreases. Under the same water depth, the Manning's roughness coefficient (n) decreases gradually with the increase in lodging angle (θ), such that $n_{20°} > n_{40°} > n_{60°} > n_{80°}$.
2. By laterally comparing the relationships shown in n–h curves under different slopes (Fig. 2b–g), it can be concluded that as the slope increases, the n–h curves appear to converge, and the degree of convergence gradually increases. In addition, the water depth can be reached under the same discharge range decreases, and the effect of the slope gradient on the roughness coefficient of lodged vege-

tation increases gradually. This process is mainly controlled by three factors: the lodging angle, slope, and water depth.

3. By longitudinally comparing the *n*–*h* relationship at a fixed lodging angle (Fig. 3), it can be concluded that with increasing water depth, the Manning's roughness coefficient (*n*) generally increases when the lodging angle is 20°. Under the same water depth, the Manning's roughness coefficient (*n*) increases as the slope increases at shallow water depths, but decreases with increases in slope at greater water depths.

It should be noted that our conclusions were derived by controlling many factors. To simplify the study, uniform vegetation heights and stem diameters were used, and four representative lodging angles and seven slope classes were selected. Therefore, the conclusions of this study are representative, but the reliability and adaptability of their application warrant further exploration.

Acknowledgements We would like to thank the National Natural Science Foundation of China (Grant No. 41471025), Postgraduate Science and Technology Innovation Project of Shandong University of Science and Technology in 2018 (Grant No. SDKDYC180320) for funding support. We would also like to thank the people in the project group for their help and support.

References

Abrahams AD, Parsons AJ (1994) Hydraulics of interrill overland flow on stone-covered desert surfaces. CATENA 23(1–2):111–140. https://doi.org/10.1016/0341-8162(94)90057-4

Atkinson JF, Abrahams AD, Krishnan C et al (2000) Shear stress partitioning and sediment transport by overland flow. J Hydraul Res 31(10):2593–2602. https://doi.org/10.1080/00221680009498356

Barros AP, Colello JD (2001) Surface roughness for shallow overland flow on crushed stone surfaces. J Hydraul Eng-ASCE 127(1):38–52. https://doi.org/10.1061/(ASCE)0733-9429(2001)127:1(38)

Busari AO, Li CW (2015) A hydraulic roughness model for submerged flexible vegetation with uncertainty estimation. J Hydro-Environ Res 9(2):268–280. https://doi.org/10.1016/j.jher.2014.06.005

Carroll C, Halpin M, Burger P et al (1997) The effect of crop type, crop rotation, and tillage practice on runoff and soil loss on a vertisol in central queensland. Aust J Soil Res 35(4):925–939. https://doi.org/10.1071/S96017

Cerdà A (1997) Soil erosion after land abandonment in a semiarid environment of southeastern spain. Arid Soil Res Rehabil 11(2):163–176. https://doi.org/10.1080/15324989709381469

Cerdà A (1997) The effect of patchy distribution of Stipa tenacissima L. on runoff and erosion. J Arid Environ 36(1):37–51. doi:10.1006/jare.1995.0198

Cheng NS, Nguyen HT (2011) Hydraulic radius for evaluating resistance induced by simulated emergent vegetation in open-channel flows. J Hydraul Eng-ASCE 137(137):995–1004. https://doi.org/10.1061/(ASCE)HY.1943-7900.0000377

Fattet M, Fu Y, Ghestem M et al (2011) Effects of vegetation type on soil resistance to erosion: Relationship between aggregate stability and shear strength. CATENA 87(1):60–69. https://doi.org/10.1016/j.catena.2011.05.006

Ferro V, Termini D, Carollo FG (2005) Flow resistance law in channels with flexible submerged vegetation. J Hydraul Eng-ASCE 131(7):554–564. https://doi.org/10.1061/(ASCE)0733-9429(2005)131:7(554)

Guo JY, Mu DP, Liu X et al (2016) Water storage changes over the tibetan plateau revealed by GRACE mission. Acta Geophys 64(2):463–476. https://doi.org/10.1515/acgeo-2016-0003

Han LJ, Zeng YH, Chen L et al (2016) Lateral velocity distribution in open channels with partially flexible submerged vegetation. Environ Fluid Mech. https://doi.org/10.1007/s10652-016-9485-9

Heuperman A (2007) Hydraulic gradient reversal by trees in shallow water table areas and repercussions for the sustainability of tree-growing systems. Agric Water Manag 39(2–3):153–167. https://doi.org/10.1016/S0378-3774(98)00076-6

Hogarth WL, Parlange JY, Rose CW et al (2005) Interpolation between Darcy-Weisbach and Darcy for laminar and turbulent flows. Adv Water Resour 28(10):1028–1031. https://doi.org/10.1016/j.advwatres.2004.10.012

Hsieh T (1964) Resistance of cylindrical piers in open-channel flow. J Hydraul Div 90(1):161–173

Hu XY, Yang YF, Shen XX (2012) Experimental study on flow velocity in open channel with different arrangement submerged flexible vegetation. Adv Mater Res 516:1093–1099. https://doi.org/10.4028/www.scientific.net/AMR.516-517.1093

Huthoff F, Augustijn DCM, Hulscher SJMH (2007) Analytical solution of the depth-averaged flow velocity in case of submerged rigid cylindrical vegetation. Water Resour Res 43(6):129–148. https://doi.org/10.1029/2006WR005625

Järvelä J (2002) Flow resistance of flexible and stiff vegetation: a flume study with natural plants. J Hydrol 269(1–2):44–54. https://doi.org/10.1016/S0022-1694(02)00193-2

Kothyari UC, Hayashi K, Hashimoto H (2009) Drag coefficient of unsubmerged rigid vegetation stems in open channel flows. J Hydraul Res 47(6):691–699. https://doi.org/10.1080/00221686.2010.529303

Liu Q, Yasufuku N, Omine K (2018) Self-watering system for arid area: a method to combat desertification. Soils Found 58(4):838–852. https://doi.org/10.1016/j.sandf.2018.03.013

Luo RT, Zhang GH, Cao Y (2009) Progress in the research of hydrodynamic characteristics of sediment-laden overland flow. Prog Phys Geog 28(4):567–574

Nouwakpo SK, Huang C, Bowling L et al (2010) Impact of vertical hydraulic gradient on rill erodibility and critical shear stress. Soil Sci Soc Am J 74(6):1914–1921. https://doi.org/10.2136/sssaj2009.0096

Querner EP (1997) Flow resistance and hydraulic capacity of water courses with aquatic weed growth. Part 2. Irrig Drain Syst 11(2):171–184. doi:10.1023/A:1005751704089

Rouhipour H, Rose CW, Yu B et al (1999) Roughness coefficients and velocity estimation in well-inundated sheetand rilled overland flow without strongly eroding bed forms. Earth Surf Proc Land 24(3):233–245. https://doi.org/10.1002/(SICI)1096-9837(199903)24:3%3c233:AID-ESP949%3e3.0.CO;2-T

Smith MW, Cox NJ, Bracken LJ (2007) Applying flow resistance equations to overland flows. Prog Phys Geogr 31(4):363–387. https://doi.org/10.1023/B:APPL.0000004932.81261.40

Vatankhah AR, Ghafari S, Mazdeh AM (2015) New and improved hydraulic radius for channels of the second kind. Ain Shams Eng J 6(3):767–773. https://doi.org/10.1016/j.asej.2015.02.003

Velasco D, Bateman A, Redondo JM et al (2003) An open channel flow experimental and theoretical study of resistance and turbulent characterization over flexible vegetated linings. Flow Turbul Combust 70(1–4):69–88. https://doi.org/10.1023/B:APPL.0000004932.81261.40

Wang XK, Yan XF, Zhou SF et al (2014) Longitudinal variations of hydraulic characteristics of overland flow with different roughness. J Hydrodyn 26(1):66–74. https://doi.org/10.1016/S1001-6058(14)60008-1

Wilson CAME, Stoesser T, Bates PD et al (2003) Open channel flow through different forms of submerged flexible vegetation. J Hydraul Eng-ASCE 129(11):750–750. https://doi.org/10.1061/(ASCE)0733-9429(2003)129:11(847)

Yagci O, Tschiesche U, Kabdasli MS (2010) The role of different forms of natural riparian vegetation on turbulence and kinetic energy characteristics. Adv Water Resour 33(5):601–614. https://doi.org/10.1016/j.advwatres.2010.03.008

Zhang ST, Zhang JZ, Liu YC et al (2018) The effects of vegetation distribution pattern on overland flow. Water Environ J. https://doi.org/10.1111/wej.12341

Zhao YY, Lu ZH, Liu JT et al (2017) Flora characteristics of Chenier Wetland in Bohai Bay and biogeographic relations with adjacent wetlands. Front Earth Sci 11:620–628. https://doi.org/10.1007/s11707-016-0599-7

Zheng FL, Huang CH, Norton LD (2000) Vertical hydraulic gradient and run-on water and sediment effects on erosion processes and sediment regimes. Soil Sci Soc Am J 64(1):4–11. https://doi.org/10.2136/sssaj2000.6414

Zhu HC, Zhao YP, Liu HY (2018) Scale characters analysis for gully structure in the watersheds of loess landforms based on digital elevation models. Front Earth Sci 12:431–443. https://doi.org/10.1007/s11707-018-0696-x